Drug Delivery and Translational Research
https://doi.org/10.1007/s13346-023-01306-x

ORIGINAL ARTICLE

Milk-derived exosomes carrying siRNA-KEAP1 promote diabetic wound healing by improving oxidative stress

Xuejiao Xiang[1] · Jing Chen[1] · Tao Jiang[1] · Chengqi Yan[1] · Yu Kang[1] · Maojie Zhang[1] · Kaituo Xiang[1] · Jiahe Guo[1] · Guoyong Jiang[1] · Cheng Wang[1] · XiangXu[1] · Xiaofan Yang[1] · Zhenbing Chen[1]

Accepted: 30 January 2023

Abstract
Diabetic wounds are a serious complication of diabetes mellitus (DM) that can lead to persistent infection, amputation, and even death. Prolonged oxidative stress has been widely recognized as a major instigator in the development of diabetic wounds; therefore, oxidative stress is considered a promising therapeutic target. In the present study, Keap1/Nrf2 signaling was confirmed to be activated in streptozotocin (STZ)-induced diabetic mice and methylglyoxal (MGO)-treated human umbilical vein endothelial cells (HUVECs). Knockdown of Keap1 by siRNA reversed the increase in Keap1 levels, promoted the nuclear translocation of Nrf2, and increased the expression of HO-1, an antioxidant protein. To explore therapeutic delivery strategies, milk-derived exosomes (mEXOs) were developed as a novel, efficient, and non-toxic siRNA carrier. SiRNA-Keap1 (siKeap1) was loaded into mEXOs by sonication, and the obtained mEXOs-siKeap1 were found to promote HUVEC proliferation and migration while relieving oxidative stress in MGO-treated HUVECs. Meanwhile, in a mouse model of diabetic wounds, injection of mEXOs-siKeap1 significantly accelerated diabetic wound healing with enhanced collagen formation and neovascularization. Taken together, these data support the development of Keap1 knockdown as a potential therapeutic strategy for diabetic wounds and demonstrated the feasibility of mEXOs as a scalable, biocompatible, and cost-effective siRNA delivery system.

Keywords Milk-derived exosomes · siKeap1 · Diabetic wound · Reactive oxygen species

Introduction

Diabetes mellitus is a major global health issue, with a rapidly increasing incidence worldwide [1]. Diabetic wounds are a major contributor to diabetes-related morbidity, as they can lead to persistent infection, amputation, and even death. Previous findings revealed that the pathological characteristics of chronic wounds that fail to heal include a reduction in the contraction of open wounds, decreased number of polymorphonucleocytes and fibroblasts, impaired neovascularization, and increased edema. Moreover, excessive and uncontrolled oxidative stress is a key pathogenic mechanism responsible for the development of diabetic wounds.

✉ Xiaofan Yang
2017xh0119@hust.edu.cn

✉ Zhenbing Chen
zbchen@hust.edu.cn

[1] Department of Hand Surgery, Union Hospital, Tongji Medical College, Huazhong University of Science and Technology, Wuhan 430022, China

Under hyperglycemic conditions, an imbalance between free radical production and cellular antioxidant defense capacity results in the accumulation of reactive oxygen species (ROS) and, subsequently, oxidative stress [2]. Many studies have shown that several oxidative stress-related pathways in the high-glucose environment are dysregulated. For example, one study demonstrated that the macrophages of diabetic rats have impaired nuclear factor erythroid-2-related factor-2 (Nrf2) activity. Nrf2 is a key transcription factor that regulates the expression of phase II detoxifying enzymes and antioxidant genes, and decreased Nrf2 activity resulted in increased ROS production and downregulation of Nrf2 target genes (including NQO-1 and HO-1). Therefore, rescuing Nrf2 activity would ameliorate oxidative stress phenotypes associated with diabetes. Kelch-like ECH-associated protein1 (Keap1) is a Nrf2 cytoplasmic repressor, and its inhibition increases Nrf2 nuclear translocation and antioxidant gene expression while decreasing ROS production. Hence, we hypothesize that the reduction of Keap1 expression by siRNA treatment can rescue oxidative stress injury

Published online: 07 February 2023

in diabetic wounds [3, 4]. Nucleic acid therapy has shown great potential for the treatment of numerous diseases, such as genetic disorders, cancer, and infection. For example, previous studies have found that the establishment of an siRNA conjugate platform enabled successful subcutaneous delivery of siRNA targeting the Marburg virus nucleoprotein [5–7].

However, the biological utility of siRNA is limited by its negative charge, instability in blood circulation, and immunogenicity. Today, while commercially available LIP3000 has been used to transfect siRNA in experimental research, it has strong toxic side effects. Therefore, there is an urgent need to develop an ideal carrier that can protect siRNA from degradation to achieve a better wound healing effect [8].

Milk-derived exosomes (mEXOs) are a type of extracellular vesicle that has attracted much attention due to their biocompatibility and suitability for scale-up technologies. The natural ability of exosomes to participate in intercellular communication can be exploited for drug delivery [9]. Specifically, the membrane structure of mEXOs is crucial to preserving its cargo as it protects nucleic acid drugs from degradation in the gastrointestinal tract and enhances drug absorption [10]. Moreover, mEXOs can be synthesized with high output and are more easily accessible compared with exosomes derived from other sources. Therefore, mEXOs exhibit several advantages that strongly support their development as nucleic acid drug delivery carriers [11].

Materials and methods

Cell culture and transfected

Human umbilical vein endothelial cells (HUVECs, #GDC166, CCTCC) were acquired from China type collection center (CCTCC, Wuhan, China) and cultured in high-glucose Dulbecco's modified eagle's medium (DMEM; supplemented with 10% fetal bovine serum (FBS; GIBCO, USA). The siKeap1 (siKeap1-1, siKeap1-2, siKeap1-3) and the relevant negative control (siNC) were obtained from Hanheng Biotechnology Company (Shanghai, China). The sequences are shown in S1. HUVECs were transfected using riboFECT™CP reagent according to the manufacturer's instructions.

RT-PCR

Total RNA was isolated using the ultrapure RNA kit (CW0581M, CWBIO), according to the manufacturer's instructions. Using a PrimeScript® RT kit (#RR037A, TaKaRa), total RNA was reversed transcribed into cDNA. On the StepOnePlus™ platform (Applied Biosystems, USA), real-time quantitative PCR (qPCR) was performed using a TB Green® Premix Ex Taq™ II kit (#RR820A, TaKaRa). The primer sequences are shown in S2. Using the $2^{-\Delta\Delta Ct}$ method, the relative expression level of target genes was calculated and normalized to β-actin.

HUVECs proliferation, migration, and intracellular ROS assessment

HUVECs from different treatment groups were grown in 96-well culture plates. After incubation with EdU, the proliferation rates of HUVECs from different groups were evaluated with the Cell-Light EdU Apollo In Vitro Kit (Ribobio, Guangzhou, China). Cell migration was assessed using the scratch test to measure the scratch closure rate. When 95% confluence was reached, the HUVEC monolayers from different groups were scraped to form a wound, and microscope images were taken. The transfected HUVECs were treated with MGO, and intracellular ROS levels were determined using DCFH-DA according to the manufacturer's instructions. All the above images were processed with Image J.

Western blot

Total protein was extracted with RIPA lysis buffer containing protease inhibitor and phosphatase inhibitor (Roche, Switzerland). Equal amounts of total protein (20–50 μg) were separated by SDS-PAGE (Beyotime Biotechnology, Shanghai, China) and then incubated overnight with primary antibodies specific for Keap1 (Proteintech, China), HO-1 (Proteintech, China), Nrf2 (Proteintech, China), β-actin (Proteintech, China), CD9 (Abcame, USA), TSG101 (ABclonal, China), or Calnexin (Abcame, USA). The membrane was incubated with secondary antibodies (Aspen, China) and exposed to X-ray film (UVP, USA). The blots were analyzed using Image J.

Extraction of milk-derived exosomes

Milk-derived exosomes (mEXOs) were extracted by differential centrifugation from commodity raw milk using previously described protocols [11]. Raw milk was centrifuged at 13,000 × *g* for 30 min at 4 °C to remove fat globules. The fat layer and particles on the bottom of the tube were discarded, and the supernatant was collected. The supernatant was ultra-centrifuged at 100,000 × *g* for 60 min to remove precipitates and large vesicles. The supernatant was ultra-centrifuged at 145,000 × *g* for 90 min to extract exosomes. The exosome pellets were washed 3 times with sterile PBS and stored at – 80 °C until use.

Ultrasonic technology

The mEXOs were loaded with siRNA-Keap1 or siRNA-FAM by sonication using the Sonics & Materials Inc. (Newtown, USA) ultrasonic system. The mEXOs and siKeap1 were mixed in a ratio of 1:1 (mass/mass) in PBS, and the final concentration of mEXOs in the mixture was 4 μg/ml. The sonication settings [12] were: 20% amplitude, 6 on/off cycles of 30 s, with a cooling time of 2 min between each cycle. After sonication, the unencapsulated siKeap1 in the supernatant was measured using a microplate reader at 260 nm, and the siKeap1 load was calculated by the weight ratio of encapsulated siKeap1 to the nanovesicles loaded with siKeap1 [13]. Then, the solution was incubated at 37 °C for 60 min to restore the exosome membrane. Where possible, the solution was placed at 4 °C before use.

Confocal microscope

The mEXOs were incubated with a red fluorescent dye (Dil, Biotium, USA) for 10 min in sterile PBS, and then, the excess dye was removed by ultra-ionization to obtain labeled mEXOs. The FAM-labeled siRNA was obtained from Hanheng Biotechnology Company (Shanghai, China) and encapsulated into Dil-mEXOs through sonication. The sequences are shown in S1. The HUVECs were seeded in 24-well culture plates and allowed to adhere and then co-cultured with Dil-mEXOs-FAM-siRNA. After incubation, HUVECs were washed twice with PBS and stained with DAPI (Solarbio, Beijing, China). The uptake of Dil-mEXOs@FAM-siRNA by HUVECs was observed by confocal microscopy.

*T*he function of mEXOs-siKeap1 complex in vitro

The diabetic cell model was achieved using methylglyoxal (MGO). Experimental groups included the control group, MGO group, MGO + siNC group, MGO + siKeap1 group, MGO + mEXOs group, and MGO + mEXOs-siKeap1 group. The procedures for the measurement of cell proliferation, migration, and ROS were performed as described above. When the HUVECs attained 30–50% confluency, the mEXOs-siKeap1 (4 μg per well) complex was added. After incubation, the acquisition and observation of images were performed as described above.

Animals' experiment

All animal experiments were approved by the Animal Protection Committee of Tongji Medical College (IACUC Number:2789). Six-week-old male C57BL/6 mice were injected intraperitoneally with streptozotocin (STZ) at 50 mg/kg daily for 5 days. The blood glucose was measured using a blood glucose monitor after 4 weeks. Blood glucose readings above 16.7 mM indicated that diabetes was induced successfully. Forty mice (including 8 normal mice and 32 diabetic mice) were anesthetized with sodium pentobarbital (Sigma-Aldrich) (1%, 50 mg/kg). After completion of back depilation and sterilization, all mice were subjected to full-thickness excision of wounds with a diameter of 10 mm. The 32 diabetic mice were randomly divided into 4 groups: PBS (STZ control) group, mEXOs (2 μg/wound), siKeap1 (2 μg/wound), and mEXOs-siKeap1 (2 μg/wound). The 8 normal mice constituted a PBS (normal control) group. After the injury, the wounds were treated at 0, 4, 9, and 14 days post-wounding. Photos were taken at days 0, 4, 9, 14, and 19 post-wounding. The wound area was measured using Image J.

Histological analysis

Nineteen days post-injury, the whole wound bed of the mice in each group was taken for histological analysis. Skin tissues from diabetic and normal mice were stored at room temperature for histology or – 80 °C for western blot analysis. The wound tissue was fixed with 4% paraformaldehyde. After dehydration, the tissue was embedded in paraffin and cut into 8-μm-thick longitudinal sections and stained. The re-epithelialization rate of wound tissue was analyzed by hematoxylin–eosin (H&E) staining, and the collagen accumulation was evaluated by Masson staining.

Immunohistochemistry and immunofluorescence analysis

To evaluate the vascular regeneration of wound beds, the skin samples collected from mice on day 19 were fixed in 4% paraformaldehyde, paraffin-embedded, and sectioned. Then, the sections were incubated overnight at 4 °C with primary antibodies against CD34 (Abcam, USA) and α-SAM (Proteintech, Wuhan, China). On the next day, the sections were incubated with a secondary antibody (Aspen, China) at room temperature. To detect the expression of the Keap1 and HO-1 (Proteintech, Wuhan, China) proteins in diabetic wound beds, we performed the corresponding immunofluorescence staining. Images were obtained using a fluorescence microscope, and four different fields were randomly assessed. Finally, ImageJ software was used for analysis.

Statistics

As more than two groups were compared, one-way analysis of variance (ANOVA) was performed with Tukey's post-hoc test. All statistical analyses were performed using GraphPad Prism software (version 8.0.2, La Jolla, CA, USA). Data are expressed as the mean ± standard deviation (SD). Statistical significance was set as $p < 0.05$ (*p < 0.05, **p < 0. 01, ***p < 0. 001, ****p < 0.0001).

Result

Knockdown of Keap1 promotes HUVEC function in MGO environment

To investigate the expression of the Keap1/Nrf2 pathway in diabetic wounds, we analyzed the content of Keap1 in a diabetic mouse model. Western blot analysis showed an upregulation of Keap1 protein in diabetic wounds (Fig. 1A). For siRNA knockdown experiments, three different siRNAs against Keap1 were transfected into HUVECs. Through qPCR (SF1) and western blot analysis (Fig. 1B), we found that siKeap1-1 had the strongest knockdown effect; cells transfected with siKeap1-1 also had the highest expression

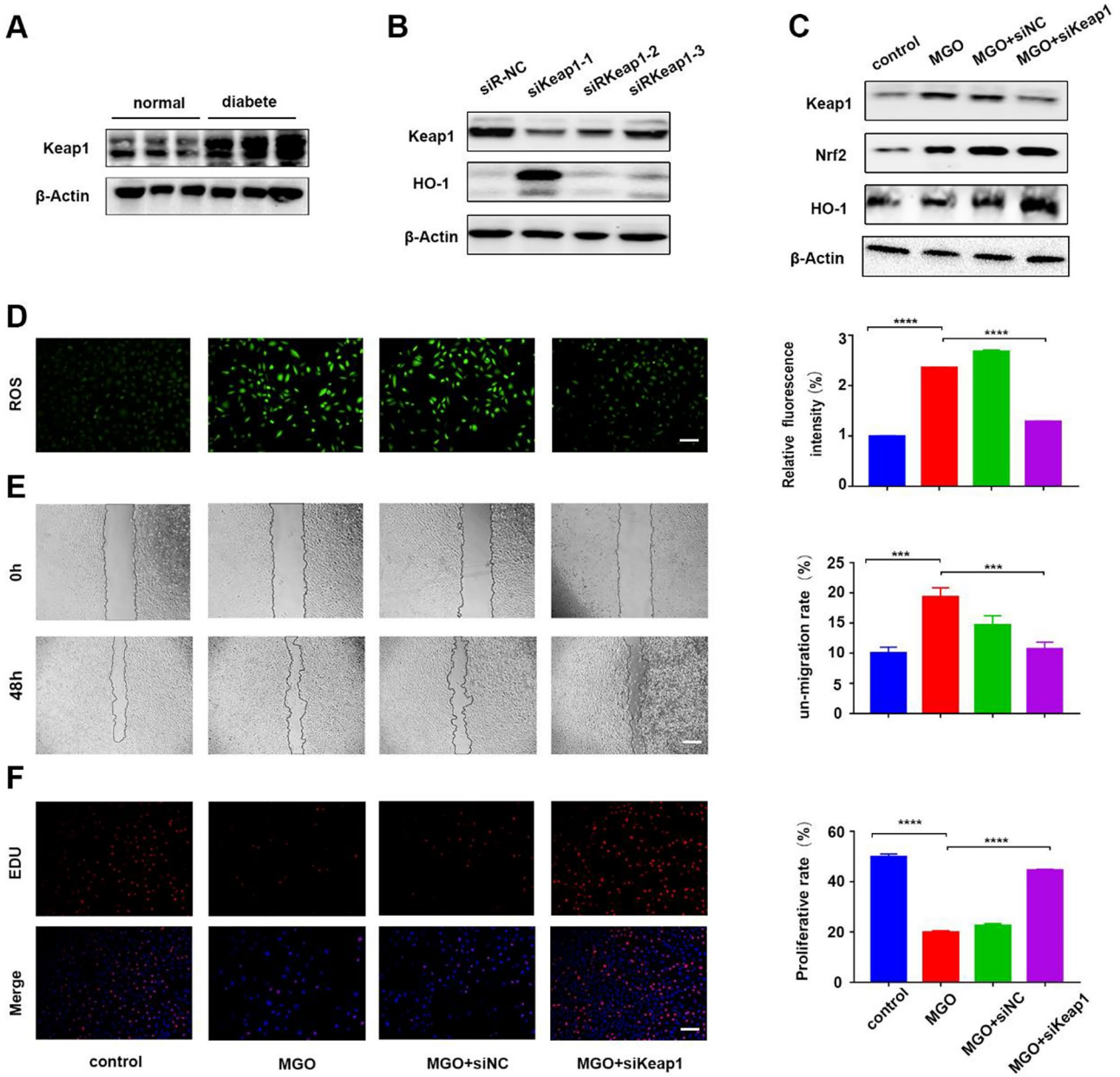

Fig. 1 Knockdown of Keap1 promotes HUVEC function in an MGO-rich environment. **A** The expression of Keap1 protein in skin samples from a mouse model of diabetic wounds. **B** Western blot analysis of the knockdown efficiency of siKeap1. **C** Western blot analysis of the Keap1/Nrf2/HO-1 pathway in HUVECs in different treatment groups. **D** Intracellular ROS level of HUVECs in each group. $n=3$, ****$p<0.0001$ vs. MGO. Scale bar, 50 μm. **E** Images of migrated HUVECs in each group. $n=3$, **$p<0.01$ vs. MGO. Scale bar, 250 μm. **F** EDU assay analysis of the proliferation rate of the HUVECs. The proliferative cells and cellular nuclei were stained with red and blue, respectively. $n=3$, ****$p<0.0001$ vs. MGO by one-way ANOVA. Scale bar, 100 μm. Data is presented as mean ± SD

of the antioxidant protein HO-1. Therefore, siKeap1-1 was chosen for subsequent experiments.

To further investigate the functional effects of Keap1 on HUVECs in a diabetic environment, a cell model of diabetes was established using MGO. Western blot analysis showed that the expression of Keap1 in the MGO group was significantly upregulated compared with the control. Meanwhile, Keap1 protein expression was decreased, and HO-1 protein was increased in the MGO + siKeap1 group (Fig. 1C). To assess oxidative stress, intracellular ROS levels were measured using the DCFH assay. We found that the MGO-only treatment group showed the highest green fluorescence intensity, indicating significant elevation in intracellular ROS levels. After transfection with siKeap1, the intracellular ROS levels in HUVECs showed significant attenuation compared with the MGO group (Fig. 1D). HUVEC proliferation was determined by EDU assay, and there were significantly more EDU-positive cells in the siKeap1 group, indicating that siKeap1 could improve the proliferation of MGO-treated HUVECs (Fig. 1F). Similarly, the migration rate of HUVECs in the siKeap1 treatment group was significantly higher than those in the MGO group and the siNC treatment group (Fig. 1E).

In conclusion, these data suggested that the upregulation of Keap1 in diabetic mice may be one of the reasons for delayed wound healing, and knockdown of Keap1 could improve the proliferation and migration of MGO-treated HUVECs, while decreasing intracellular ROS levels.

Characterization of mEXOs and mEXOs-siKeap1

To synthesize an ideal delivery vector, mEXOs were extracted by differential centrifugation from raw milk. Transmission electron microscopy (TEM) showed nanoparticles wrapped by a typical lipid bilayer film (Fig. 2A). Moreover, nanoparticle tracking analysis (NTA) showed

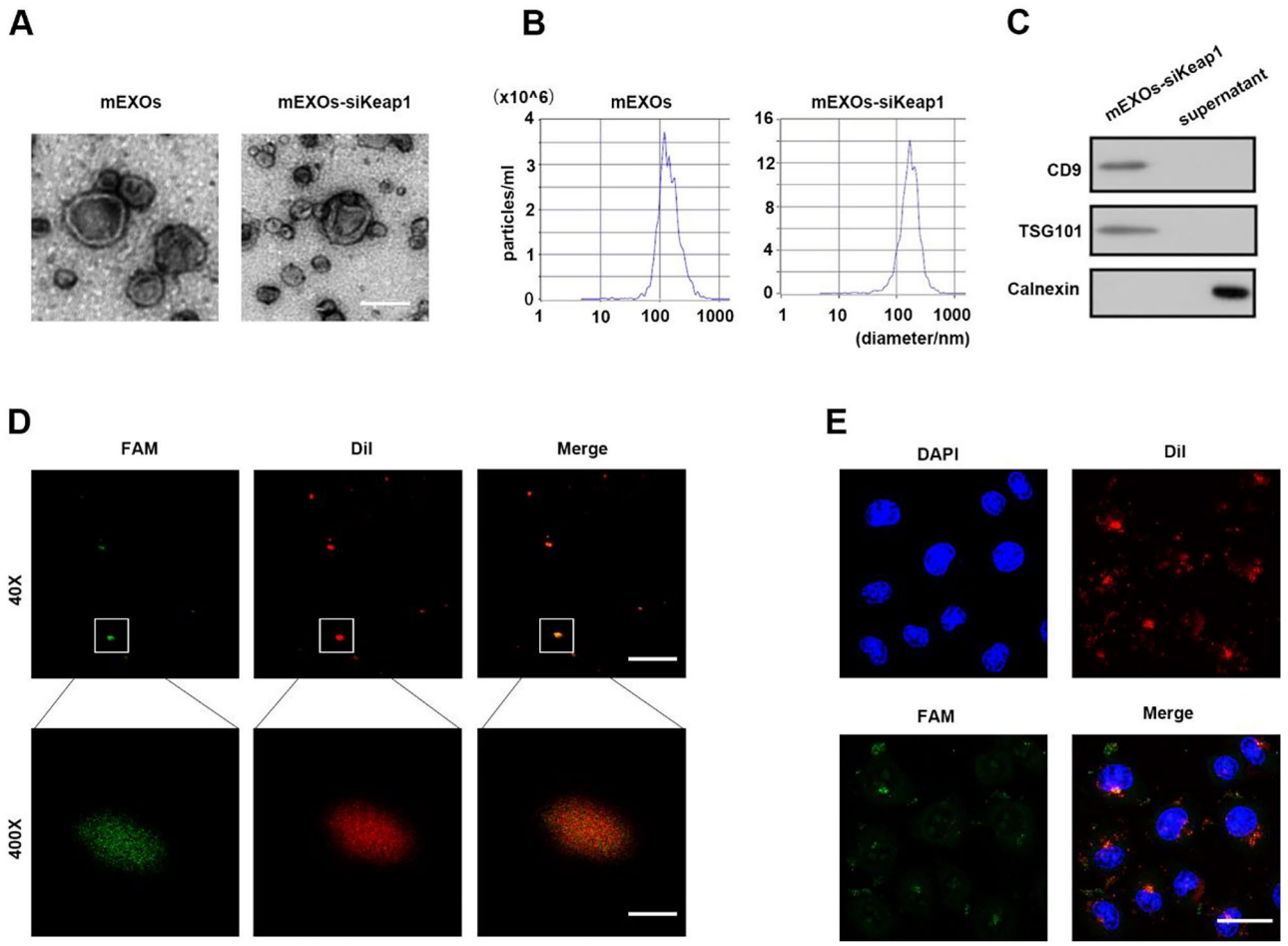

Fig. 2 Characterization of mEXOs and mEXOs-siKeap1. **A** TEM images showing the morphology of mEXOs. Scale bar, 100 nm. **B** NTA results showing the size distribution of mEXOs. **C** Western blotting analysis of exosomal markers CD9 and TSG101. **D** Confocal microscopy analysis reveals that the mEXOs-siKeap1 were successfully synthetized. Red and green fluorescence represents mEXOs and siKeap1, respectively. Scale bar, 100 μm (40×) and 10 μm (400×). **E** The uptake of mEXOs-siKeap1 by HUVECs. Scale bar, 50 μm

that the peak diameters of mEXOs and mEXOs-siKeap1 were 156.4 nm and 170.6 nm, respectively (Fig. 2B). Based on western blot analysis, the mEXOs-siKeap1 complex expressed the exosomal markers CD9 and TSG101, but not calnexin (a protein found at high levels in milk supernatant) (Fig. 2C). To explore the potential of mEXOs in siRNA delivery, we encapsulated siKeap1 in mEXOs and examined the drug loading of siRNA. As shown in Supplemental Fig. 2, siRNA was incorporated into mEXOs with a high loading efficiency of up to 24%.

In order to verify that siKeap1 was successfully loaded into mEXOs, the Dil-labeled mEXOs were loaded with FAM-labeled siKeap1 by sonication, and the obtained Dil-mEXOs@FAM-siKeap1 were observed by confocal microscopy. As shown in Fig. 2D, green fluorescent siKeap1 and red fluorescent mEXOs could merge and overlap to produce orange-yellow light, indicating that FAM-labeled siKeap1 were successfully loaded into mEXOs. To investigate the uptake of mEXOs-siKeap1 by HUVECs, HUVECs were co-cultured with Dil-mEXOs@FAM-siKeap1 for 24 h. Through confocal imaging, we found that FAM-siKeap1 was successfully internalized into the cytoplasm of HUVECs, following the mEXOs (Fig. 2E). Meanwhile, HUVECs treated with the mECOs-siKeap1 complex showed decreased levels of Keap1 protein. Therefore, we could conclude that the mEXOs-siKeap1 complex was synthetized successfully (SF3).

mEXOs-siKeap1 improves HUVEC function in vitro

To verify that mEXOs-siKeap1 could improve the function of MGO-treated HUVECs with respect to proliferation, migration, and intracellular ROS level, we treated HUVECs with different drugs as described in the method above. First, the intracellular ROS levels were measured using the DCFH assay. We found that the MGO group showed the highest green fluorescence intensity, indicating significant elevations in intracellular ROS levels. Treatment of MGO-treated HUVECs with mEXOs and free siKeap1 could not decrease the high ROS levels in the cells, but mEXOs-siKeap1 significantly reversed the increase in intracellular ROS to alleviate oxidative stress injury (Fig. 3A). Next, we evaluated the migration ability of HUVECs by cell scratch assays. The migration in the MGO group was significantly reduced compared with the control group. However, the MGO-induced impairment in HUVEC migration was reversed following treatment with mEXOs-siKeap1, indicating that mEXOs-siKeap1 treatment could protect cells to maintain normal migration function in an environment of MGO and oxidative stress (Fig. 3B). Furthermore, EdU assays were performed to assess HUVEC proliferation. The proliferation rates decreased to 10% when HUVECs were treated with MGO (Fig. 3C). In contrast, proliferation in the mEXOs-siKeap1 group was increased more than fourfold compared with the mEXOs and siKeap1 groups (Fig. 3C). In a word, mEXOs-siKeap1 can alleviate the MGO-induced increase in intracellular ROS to maintain low ROS levels, while also improving the proliferation and migration abilities of MGO-treated cells.

mEXOs-siKeap1 accelerates diabetic wound healing in vivo

To confirm that the mEXOs-siKeap1 could promote diabetic wound healing, mEXOs-siKeap1 were tested in a mouse model of wound healing. STZ-induced diabetic mice were administered PBS, mEXOs, siKeap1, or mEXOs-siKeap1 by subcutaneous injection (50 μL per mouse), while normal mice were given PBS (Fig. 4A). As shown in the Fig. 4B and C, the wound healing rate of normal mice is faster than that of diabetic mice during the whole process. However, there was no significant difference among the diabetic groups on the 4th day as this was during the initial inflammatory stage (Fig. 4B, C). As expected, the wound healing rate of diabetic mice in the mEXOs-siKeap1 group was significantly faster than that of the PBS group at days 9, 14, and 19 post-wounding. Hence, we could conclude that the mEXOs-siKeap1 treatment accelerated the wound healing rate.

H&E staining analysis showed that the mEXOs-siKeap1 treatment group exhibited the highest re-epithelialization rate among all diabetic mice (Fig. 5A). Meanwhile, Masson staining analysis showed that collagen deposition in the mEXOs-siKeap1-treated group was superior to that in the other diabetic groups (Fig. 5B). We observed no difference in collagen deposition between the siKeap1 group compared to the PBS and mEXOs groups. Two vascular markers, CD34 and α-SMA, were used to evaluate angiogenesis in diabetic wounds by immunohistochemical staining. As shown in Fig. 5C, few blood vessels are observed in the wound tissues of the PBS, mEXOs, and siKeap1 groups, with the highest vascular density in diabetic mice observed in the mEXOs-siKeap1 group (Fig. 5C). Next, immunofluorescence staining against HO-1 was performed to determine antioxidant protein expression in wound tissue. As expected, the fluorescence intensity of tissue stained with anti-HO-1 antibody was significantly enhanced in skin wound samples from diabetic mice treated with mEXOs-siKeap1 compared to the other diabetic groups (Fig. 5D). Taken together, these results revealed that the acceleration of wound healing by mEXOs-siKeap1 was associated with enhanced collagen formation and neovascularization in this mouse model.

Discussion

Oxidative stress is widely known to be associated with inflammation, and both are implicated in diabetes and other diseases. Among the cellular defenses against oxidative

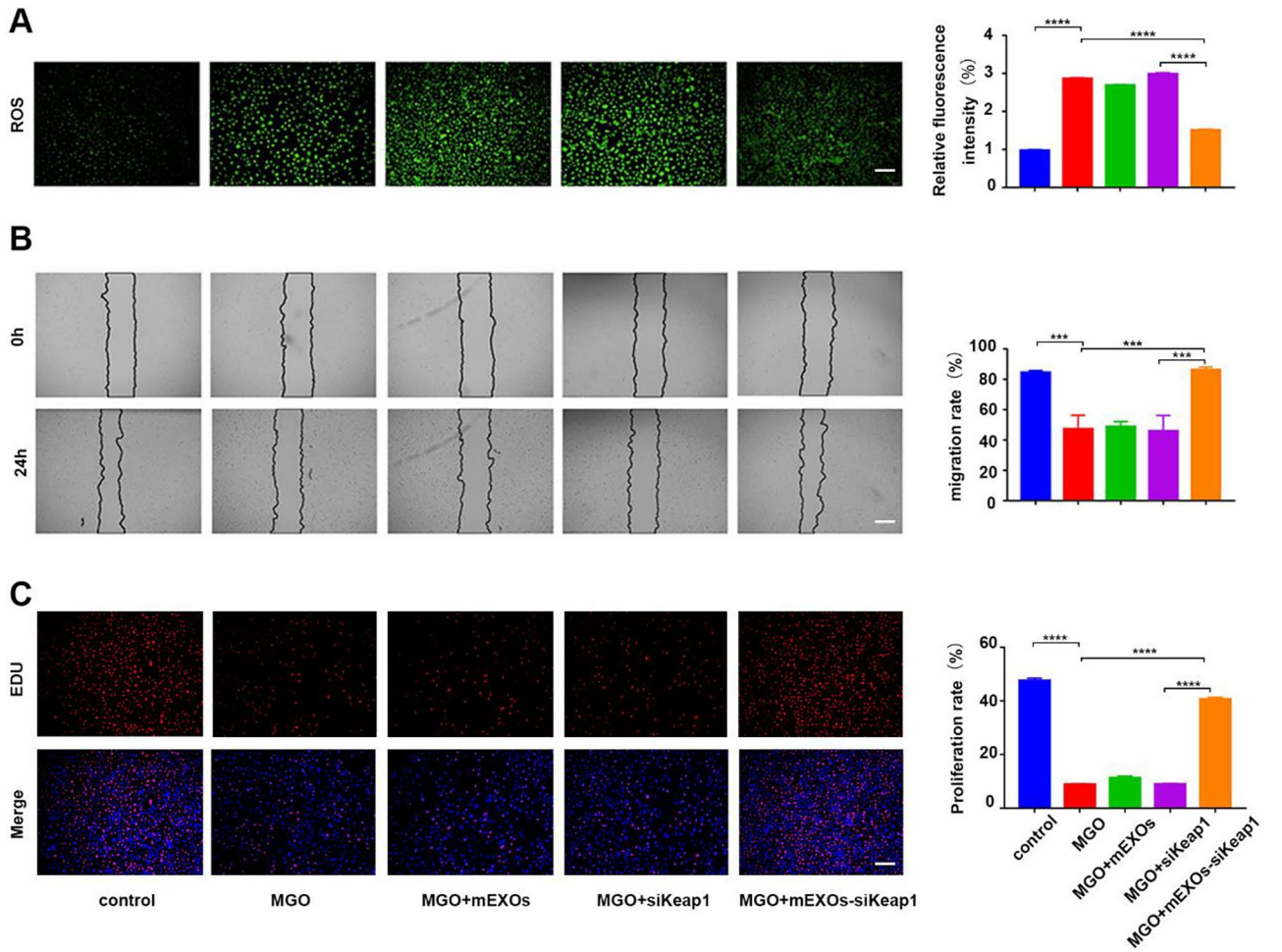

Fig. 3 mEXOs-siKeap1 improve cell function in MGO-treated HUVECs. **A** The ROS levels of HUVECs in each group. $n=3$, ****p < 0. 0001 vs. MGO. Scale bar, 50 μm. **B** Analysis of HUVEC migration by cell scratch test. $n=3$, ****p < 0.0001 vs. MGO. Scale bar, 250 μm. **C** EdU assay analysis of the proliferation rate of HUVECs. The proliferating cells and cellular nuclei were stained with red and blue fluorescence, respectively. $n=3$, ****p < 0.0001 vs. MGO by one-way ANOVA with Tukey's post-hoc test. Scale bar, 100 μm. Data are presented as mean ± SD

stress, the transcription factor Nrf2 is a critical player [14]. Nrf2 and its cytoplasmic repressor, Keap1, are master regulators under conditions of oxidative stress, which function to manage redox homeostasis, cytoprotective programming, and anti-inflammatory activities [15]. The Keap1/Nrf2 signaling pathway has been shown to be impaired in both diabetic humans and animal models of diabetes, concurrent with increased Keap1 protein [16], suggesting a central role for modulators of oxidative stress. We previously investigated the use of synthetic ADSC-exo@MMP-PEG hydrogel in wound treatment, demonstrating that it could alleviate H_2O_2-induced oxidative stress and rescue the impaired wound healing in diabetic mice [17]. Furthermore, the thermosensitive niobium carbide (Nb_2C)-based hydrogel (Nb_2C@Gel), which has antioxidant and antimicrobial activity, could promote wound healing by attenuating ROS levels [18]. A specific role of Nrf2 was highlighted in research by Simu et al., which indicated that oxidative stress could be decreased by activating Nrf2, as Nrf2 mediates ROS elimination and nitric oxide generation [19]. Therefore, based on these studies, it is reasonable that the Nrf2-related downstream genes, such as HO-1, could be upregulated by knocking down Keap1. Hence, siRNA knockdown of Keap1 is a promising strategy to accelerate diabetic wound healing by alleviating ROS levels.

Exosomes, due to its antigen-presenting properties and drug-loading properties, are widely used as drug carriers in researches [12]. In previous studies, Zhang and Liu discussed the application of exosome on drug delivery as carriers for DNA, messenger RNA, microRNA, small-interfering RNA, and other nucleic acids [20]. Exosomes were as naturally derived vesicles without production-related hurdles. Furthermore, previous studies have revealed that exosomes could cross the blood–brain barrier

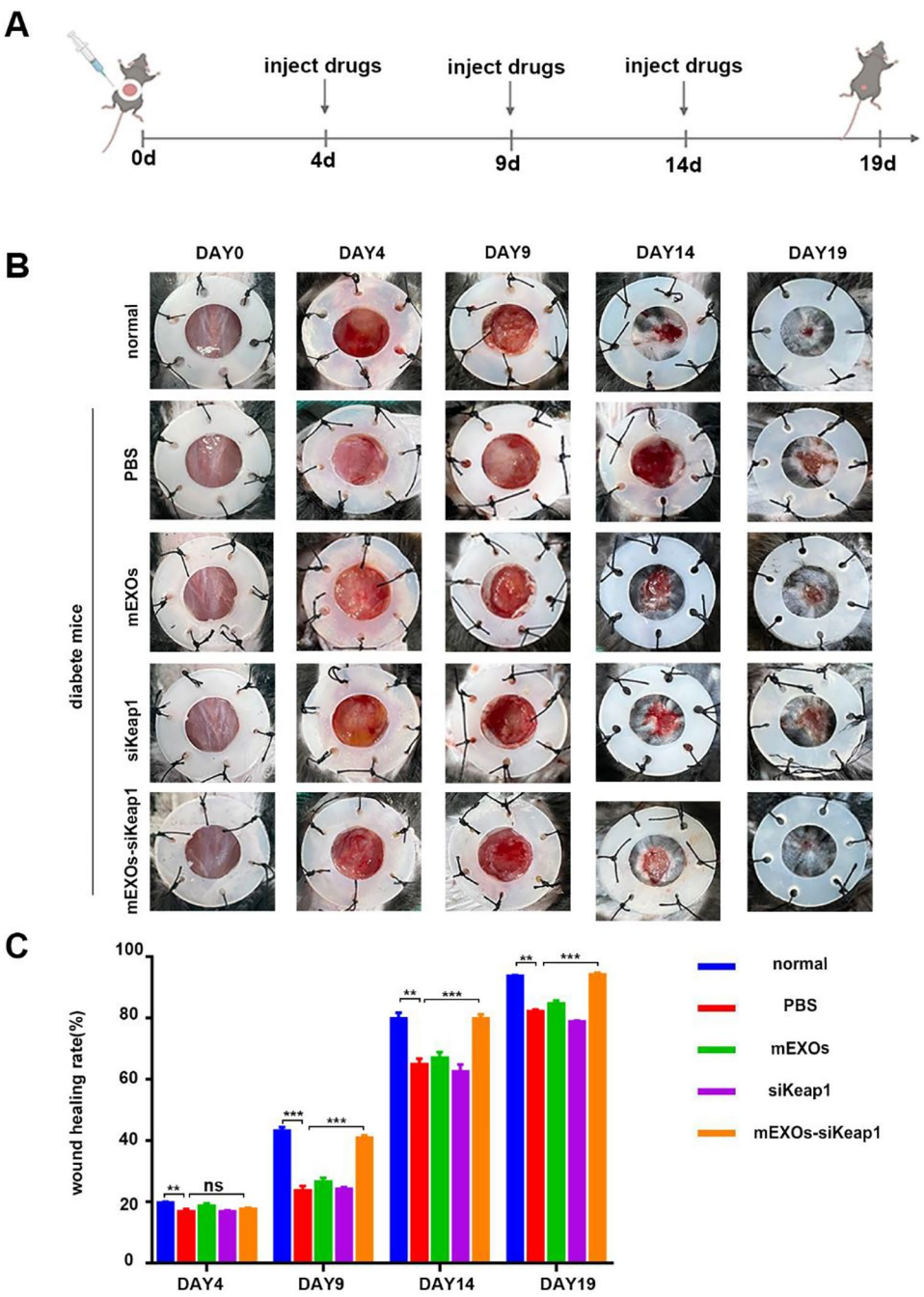

Fig. 4 mEXOs-siKeap1 accelerated diabetic wound healing in vivo. **A** The schematic diagram of treatment timeline showing time points for drug injection into skin wounds. **B**, **C** Representative images and statistics of wound closure in a wound model at the dorsum of diabetic mice at days 0, 4, 9, 14, and 19 post-wounding. $n = 5$. ***$p < 0.001$ vs. PBS by one-way ANOVA. Data are presented as mean ± SD

and maternal placental barrier. The phospholipid bilayer provided excellent membrane permeability and protects the encapsulation agent from degradation. However, the disadvantages lie in the lack of general methods for separating and collection [21]. Lipid nanoparticle (LNP) vectors, one of the most advanced non-viral drug delivery systems, were currently used in COVID-19 mRNA vaccines developed by Moderna (MRNA-1273) and Pfizer BioNTech (BNT162b2) due to the biocompatibility and immunogenicity, while the previous study had found that based on the total surface charge, liposomes are called anions, cations, and neutrals. The properties and density of the charge can be changed by adjusting the composition of the lipids used to form the liposomes. Neutral surface charges can lead to liposome aggregation and low physical stability. This can cause liposomes to escape into extracellular space because these liposomes do not interact well with cells. Negatively charged liposomes consist of anionic lipids and are reported to be more unstable than neutral or positively charged liposomes. In addition, they are quickly absorbed by the reticuloendothelial system and may also cause toxic side effects. Furthermore, the storage

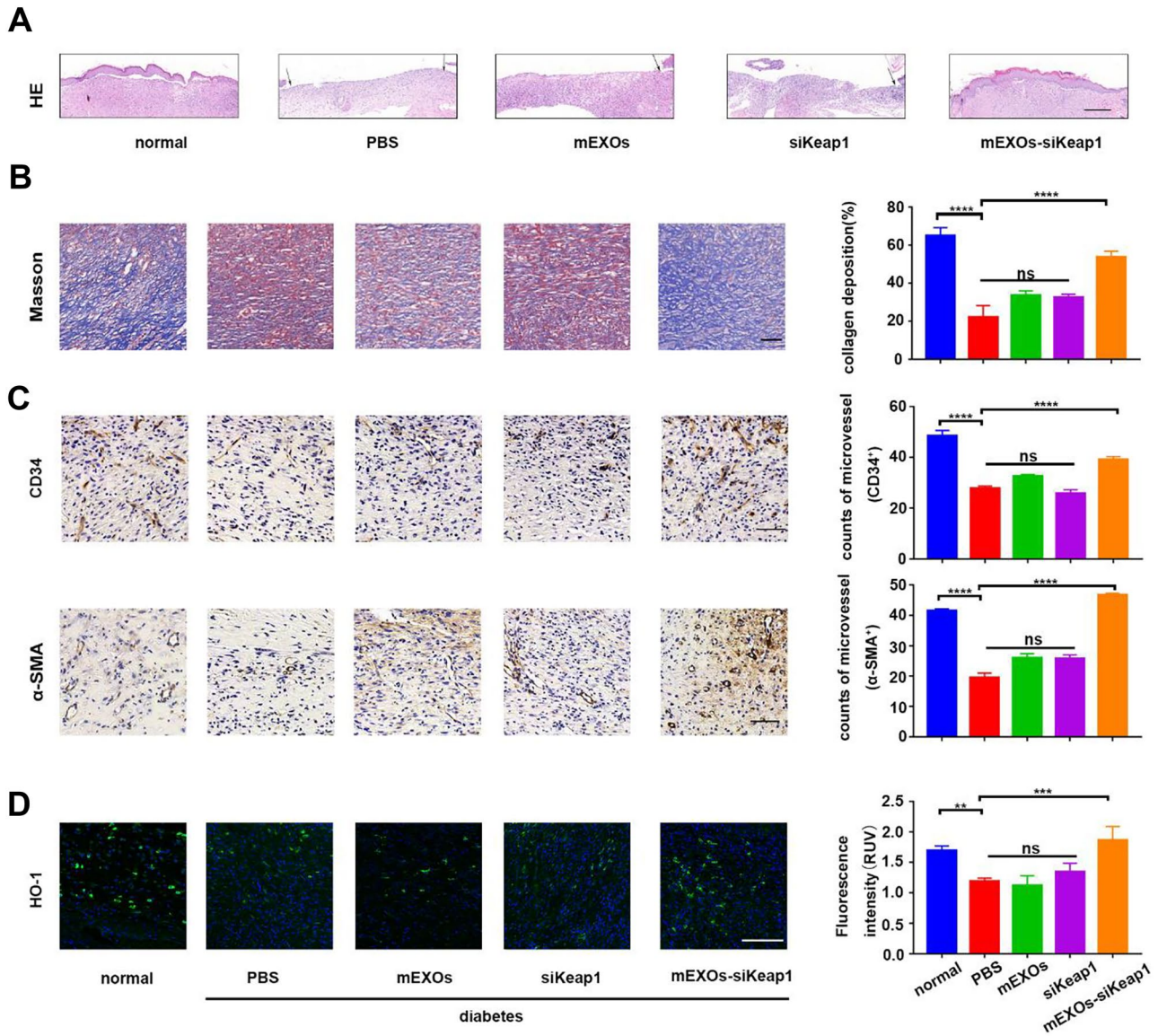

Fig. 5 Histological, immunohistochemical, and immunofluorescent analysis of wound tissues. **A** H&E staining analysis of wound sections at day 19 post-wounding. The black single-headed arrows indicate the un-epithelialized areas. Scale bar, 500 μm. **B** Masson staining for the evaluation of collagen deposition at day 19 post-wounding. ****$p < 0.0001$ vs. PBS. Scale bar, 200 μm. **C** The expression of angiogenic markers in skin wound tissue, including CD34 and α-SMA, as assessed by immunohistochemical analysis. ****$p < 0.0001$ vs. PBS. Scale bar, 100 μm. **D** Immunofluorescence staining against the antioxidant protein HO-1 at day 19 post-wounding. ***$p < 0.001$ vs. PBS by one-way ANOVA with Tukey's post-hoc test. Scale bar, 100 μm. Data are presented as means ± SD

of lipid nanoparticles was a challenge for their large-scale development [22–25].

Exosomes were found in body fluids such as urine, saliva, amniotic fluid, and ascites. Milk was the only commercially available bio-liquid containing EXO. As a rich source of EXO, milk has unique properties as a carrier [26] which had been utilized in enhancing the anticancer activity against oral squamous cell carcinoma [27] and treating the ovarian cancer [28]. On the basis of our group's previous studies, it has been reported that bovine milk-derived exosomes as a drug delivery vehicle has played an important role in miRNA-based therapy to accelerate the diabetic wound healing. Furthermore, there are several advantages of the mEXOs in higher yield, easier extraction, good stability, low immunogenicity, and good cross species tolerance [11, 29]. In this research, the mEXO-siKeap1 complex was synthesized with milk-derived exosome and siKeap1 using ultrasonic technique. The peak diameters of mEXOs and mEXOs-siKeap1 have no difference. And the mEXOs-siKeap1 complex could promote HUVEC proliferation and

migration, relieve oxidative stress, reduce the level of Keap1 protein, and increase the expression of the Nrf2 and HO-1 antioxidant protein in vitro, which were consistent with previous research results. Meanwhile, the mEXO-siKeap1 was proved to be beneficial for diabetic wound healing, collagen formation, and neovascularization in vivo. Therefore, it may be a therapy for diabetic wound delaying by delivering drugs by milk exosome.

Conclusion

The treatment of delayed wound healing in diabetes requires more multidisciplinary and proactive approaches in order to heighten patients' live quality. In this study, milk-derived exosomes were used as a desirable carrier to delivery siKeap1. And the mEXOs-siKeap1 complex which was synthetized by ultrasonic significantly could accelerate the healing process of diabetes wounds. Therefore, with rapid advances in modification technology of exosomes, the collection and storage technology of exosomes, mEXOs-siRNA, would prove to be a new means of treating diabetic wounds in prospect. Meanwhile, it proved the feasibility of mEXOs as a scalable, biocompatible, and cost-effective siRNA delivery system.

Supplementary Information The online version contains supplementary material available at https://doi.org/10.1007/s13346-023-01306-x.

Acknowledgements Scheme 1 was created with Bio Render (Biorender.com).

Author contribution Xuejiao Xiang: Conception and design, collection and/or assembly of data, data analysis and interpretation, and manuscript writing. Xiaofan Yang and Zhenbing Chen: Conceptualization, methodology, writing–review and editing, supervision, funding acquisition. Jing Chen, Tao Jiang, Chengqi Yan: Investigation, formal analysis, manuscript revision. Maojie Zhang, Kaituo Xiang, Jiahe Guo, Guoyong Jiang, Cheng Wang, XiangXu: Resources.

Funding This work was supported by the Key Research and Development Program of Hubei Province (grant number2020BCB031) and the Knowledge Innovation Project of Wuhan (grant numbers 2022020801010459 and 2022020801020463).

Availability of data and materials The authors confirm that the data supporting the findings of this study are available within the article.

Declarations

Ethical approval and consent to participate Ethical approval to conduct the study was obtained from the Ethical Committee on Animal Experiments of Huazhong University of Science and Technology (IACUC Number: 2789).

Consent for publication Not applicable.

Competing interests The authors declare no competing interests.

References

1. Ramzi Shawahna P, et al. Pharmaceutical care services for patients with diabetes: a systematic scoping review. Am J Manag Care. 2022;28(9).
2. Deng L, et al. The role of oxidative stress and antioxidants in diabetic wound healing. Oxid Med Cell Longev. 2021;2021:8852759.
3. Li M, et al. Nrf2 suppression delays diabetic wound healing through sustained oxidative stress and inflammation. Front Pharmacol. 2019;10:1099–1099.
4. Soares MA, et al. Restoration of Nrf2 signaling normalizes the regenerative niche. Diabetes. 2016;65(3):633–46.
5. Ye X, et al. Combination treatment of mannose and GalNAc conjugated small interfering RNA protects against lethal Marburg virus infection. Mol Therap. 2022.
6. Steffens RC, Wagner E. Directing the way—receptor and chemical targeting strategies for nucleic acid delivery. Pharm Res. 2022.
7. Yang G, et al. Construction of PEI-EGFR-PD-L1-siRNA dual functional nano-vaccine and therapeutic efficacy evaluation for lung cancer. Thoracic Cancer. 2022;13(21):2941–50.
8. Liu Q, et al. Mesoporous silica-coated silver nanoparticles as ciprofloxacin/siRNA carriers for accelerated infected wound healing. J Nanobiotechnol. 2022;20(1):386.
9. Ahmed F, et al. Drug loading and functional efficacy of cow, buffalo, and goat milk-derived exosomes: a comparative study. Mol Pharm. 2022;19(3):763–74.
10. Feng X, et al. Latest trend of milk derived exosomes: cargos, functions, and applications. Front Nutr. 2021;8:747294–747294.
11. Yan C, et al. Milk exosomes-mediated miR-31-5p delivery accelerates diabetic wound healing through promoting angiogenesis. Drug Delivery. 2022;29(1):214–28.
12. Hosseinikhah SM, et al. Role of exosomes in tumour growth, chemoresistance and immunity: state-of-the-art. J Drug Target. 2022;1–19.
13. Zhou X, et al. Tumour-derived extracellular vesicle membrane hybrid lipid nanovesicles enhance siRNA delivery by tumour-homing and intracellular freeway transportation. J Extracellular Vesicles. 2022;11(3).
14. Wu S, et al. Antioxidant and anti-inflammation effects of dietary phytochemicals: The Nrf2/NF-κB signalling pathway and upstream factors of Nrf2. Phytochemistry. 2022;204.
15. Iorio R, Celenza G, Petricca S. multi-target effects of ß-caryophyllene and carnosic acid at the crossroads of mitochondrial dysfunction and neurodegeneration: from oxidative stress to microglia-mediated neuroinflammation. Antioxidants (Basel, Switzerland). 2022;11(6):1199.
16. Sharp-Tawfik A, et al. Proteomic examination of Cornus officinalis stimulated 1.1B4 human pancreatic cells reveals activation of autophagy and Keap1/Nrf2 pathway. Mol Cellular Endocrinol.2022;557:111773.
17. Jiang T, et al. ADSC-exo@MMP-PEG smart hydrogel promotes diabetic wound healing by optimizing cellular functions and relieving oxidative stress. Materials today Bio. 2022;16:100365–100365.
18. Chen J, et al. Tailored hydrogel delivering niobium carbide boosts ROS-scavenging and antimicrobial activities for diabetic wound healing. Small. 2022;18(27):2201300.
19. Simu SY, Alam MB, Kim SY. The activation of Nrf2/HO-1 by 8-Epi-7-deoxyloganic acid attenuates inflammatory symptoms through the suppression of the MAPK/NF-κB signaling cascade in in vitro and in vivo models. Antioxidants (Basel, Switzerland). 2022;11(9):1765.
20. Zhang Y, et al. Recent advances in exosome-mediated nucleic acid delivery for cancer therapy. J Nanobiotechnol. 2022;20(1):279.

21. Song J, et al. Multiplexed strategies toward clinical translation of extracellular vesicles. Theranostics. 2022;12(15):6740–61.
22. Yamada Y. Nucleic acid drugs—current status, issues, and expectations for exosomes. Cancers. 2021;13(19):5002.
23. Hallan SS, et al. Lipid-based nano-sized cargos as a promising strategy in bone complications: a review. Nanomaterials. 2022; 12(7):1146.
24. Zulaikha M, et al. Pulmonary delivery of siRNA against acute lung injury/acute respiratory distress syndrome. Acta Pharmaceutica Sinica B. 2022;12(2):600–20.
25. Syama K, et al. Development of lipid nanoparticles and liposomes reference materials (II): cytotoxic profiles. Sci Rep. 2022;12(1): 18071.
26. Melnik BC, Schmitz G. Milk exosomal microRNAs: postnatal promoters of β cell proliferation but potential inducers of β cell de-differentiation in adult life. Int J Mol Sci. 2022;23(19):11503.
27. Zhang Q, et al. Milk-exosome based pH/light sensitive drug system to enhance anticancer activity against oral squamous cell carcinoma. RSC Adv. 2020;10(47):28314–23.
28. Aqil F, et al. Exosomal delivery of berry anthocyanidins for the management of ovarian cancer. Food Funct. 2017;8(11):4100–7.
29. Zhong J, et al. High-quality milk exosomes as oral drug delivery system. Biomaterials. 2021;277.